Chapter 9
Liquid Crystalline Polymers from Renewable Resources: Synthesis and Properties

K.Y. Sandhya, A. Saritha, and Kuruvilla Joseph

9.1 Introduction

Synthesis of soft matter from renewable resources has gained a great deal of attention in the current research scenario. Effective utilization of bio mass as well as biodegradable industrial by-products towards the synthesis of soft materials like liquid crystals (LCs), which have a direct impact on the life and development of humanity is indeed a challenge to the growing research community. It is believed by the scientific community that only natural resources would be a viable solution to all the technological developments in the long run and hence it would be better to replace the non renewable resources with the easily available bio resources. The fact that natural products are stereo- and regiochemically pure makes them in essence special and reduces the dependence on expensive chiral catalysts and complex synthesis that are currently mandatory for selective functionalization in chemical industry.

LC is a unique state of matter which is between the solid and the liquid state. Within solids, particles (atoms, ions, molecules) are often localized in a regular crystal lattice and crystalline solids exhibit short as well as long-range order with regard to both position and orientation of the particles. The liquid crystalline phases—also known as mesophases—represent intermediate states between the ordered structure of solids and amorphous properties of liquids. In LC, the molecules may flow like a liquid and at the same time will maintain an ordered

K.Y. Sandhya • K. Joseph (✉)
Department of Chemistry, Indian Institute of Space Science and Technology, Valiamala, Thiruvananthapuram, Kerala 695547, India
e-mail: sandhya@iist.ac.in; kjoseph.iist@gmail.com

A. Saritha
Department of Chemistry, Amrita Viswa Vidyapeetham University, Amritapuri, Kollam, Kerala 690525, India
e-mail: sarithatvla@gmail.com

V.K. Thakur, M.R. Kessler (eds.), *Liquid Crystalline Polymers*,
DOI 10.1007/978-3-319-22894-5_9

arrangement like a crystal, hence given the name "LC". LC states show at least one orientational long range order and in some cases may show short range order as well, whereas positional long-range order of crystals disappears. Many different mesophases are known for LCs and the simplest mesophase among them is the nematic phase (Fig. 9.1) where positional order is totally lost but an orientational order remains. Smectic phase has a higher positional order with a layered arrangement (Fig. 9.1) and in each layer molecules have a nematic like arrangement. When molecules are arranged perpendicular to the layers, the phase is called smectic A and when it is tilted it is a smectic C. Many other phases are exhibited by LCs such as cholesteric phase (chiral nematic phase), columnar phase, etc. and the mesophases formed mainly dependent on the structure and shape of the mesogens. Materials that are capable of transforming into the liquid crystalline phase often consist of molecules with an anisometric shape called mesogens. Other than that the parameters that govern the formation of liquid crystalline phases are the aspect ratio of the mesogen, micro segregation effect, chirality etc. In addition to this, the very well known parameter, in the case of lyotropic LCs is the solvent concentration of the material and in thermotropic LCs is the temperature that affects the formation of the LC phase (Stegemeyer 1999).

The two methods by which a crystalline solid with its ordered structure can turn into a partially disordered LC are the melting and the dissolution depending on which the LCs are classified as thermotropic and lyotropic LCs, respectively. In thermotropic LCs, as mentioned earlier, the formation of mesophases occurs via a variation in temperature whereas in lyotropic LCs, the formation of mesophases requires the presence of a solvent and they are formed by mesogens; not the molecules themselves, their solvates as well as associates of the solvated molecules (Davidson and Gabriel 2005).

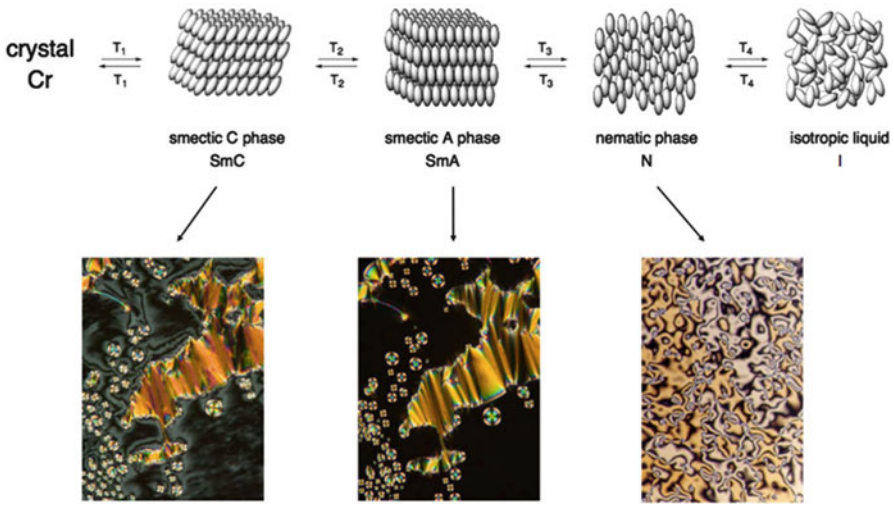

Fig. 9.1 Schematic of the molecular arrangements in various mesophases of a thermotropic LC and the corresponding representative textures

Liquid crystalline polymers (LCPs) form an important class of compounds with molecular self-orientation ability which finds application in high performance materials. LCPs have been synthesized from a large range of bio-based materials like cardanol, coconut oil, castor oil, lipids, cellulose etc. and been extracted from various natural sources. LCPs of biological origin like DNA, spider silk, polypeptides etc. are liquid crystalline in nature and the LC order is thought to play a critical role in the exceptional properties and functions of the biological structures.

Presence of molecular interactions in the system and the occurrence of semi rigid backbone contribute to the force pertaining to the formation of LCs from cellulose and its derivatives (Huang et al. 1995). Vegetable oils like coconut oil, olive oil can be used as an alternative to expensive fatty acids for the preparation of LCs because of their easy availability and low price. Aromatic polyamides derived from oils are not usually used for this purpose due to the difficulties associated with the fabrication. However to overcome this problem flexible groups are introduced in the rigid backbone of the aromatic polyamide so as to make them suitable for the preparation of liqLCPs (Abid et al. 2004). In this chapter we have tried to give a general idea about bio-based LCPs starting from the humble cardanol to the complicated biologically inspired LCPs.

9.2 Synthesis of Liquid Crystalline Polymers

9.2.1 Natural Oil Based LCPs

Cashew nut is grown extensively in the tropical regions and its shell is rich in natural long chain phenols; cardanol and cardol, which together are technically known as cashew nut shell liquid (CNSL). Cardanol the distilled product of CNSL, is a phenolic lipid which finds abundant applications in chemical industry. Cardanol has several specialties in its structure which enable it to get transformed into a number of high performance polymers and consists of four meta-alkyl phenols, with alkyl chains having different degree of unsaturation.

LCPs with cross-linked network structures containing azobenzene mesogens were synthesized from cardanol (Saminathan and Pillai 2000). They introduced the azobenzene group by the diazo coupling reaction between cardanol and 4-aminobenzoic acid. The resulting monomer, 4-[(4-cardanyl) azo] benzoic acid was polymerised by self-polycondensation using thionyl chloride and pyridine to get poly[4-[(4-cardanyl)azo]benzoic acid]. The monomer could also be converted to poly[4-[(4-acryloyloxycardanyl)azo]benzoic acid] through acryloylation, followed by free radical polymerization. Cationic polymerization of the monomer gave poly[4-[(4-cardanyl)azo]benzoic acid]. The schemes 9.1, 9.2 and 9.3 shows the preparation of the polymers from cardanol.

The phase behavior of these polymers was studied using hot stage polarized light microscope (PLM) and it was found that the poly[4-[(4-cardanyl)azo]benzoic acid] did not exhibit melting to form mesophase but started decomposing above 200 °C.

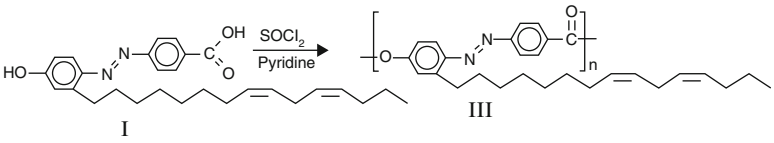

Scheme 9.1 Synthesis of poly[4-[(4-cardanyl)azo]benzoic acid]. Reproduced with permission from Saminathan and Pillai (2000). Copyright Elsevier

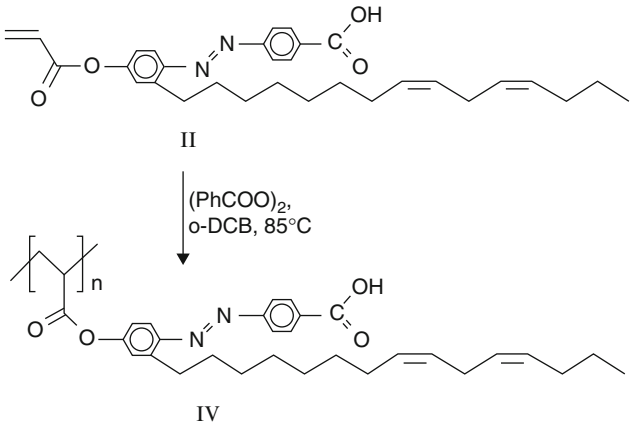

Scheme 9.2 Synthesis of poly[4-[(4-acryloyloxycardanyl)azo]benzoic acid]. Reproduced with permission from Saminathan and Pillai (2000). Copyright Elsevier

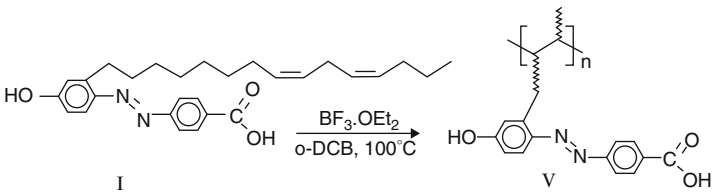

Scheme 9.3 Cationic polymerisation of 4-[(4-cardanyl)azo]benzoic acid. Reproduced with permission from Saminathan and Pillai (2000). Copyright Elsevier

On the other hand, the sample prepared by rapid melting below the decomposition temperature and quenching to room temperature showed threaded nematic texture. The polymer poly[4-[(4-acryloyloxycardanyl)azo]benzoic acid] melted at 153 °C exhibiting a clear schlieren texture (Fig. 9.2b) characteristic of nematic phase under PLM. The unsaturated C15 hydrocarbon side chain in cardanol is utilized for cross-linking reactions.

Castor oil contains a dicarboxylic acid of 36 carbon atoms, called dimer acid, which functions as an excellent precursor for LCPs in conjunction with aliphatic as

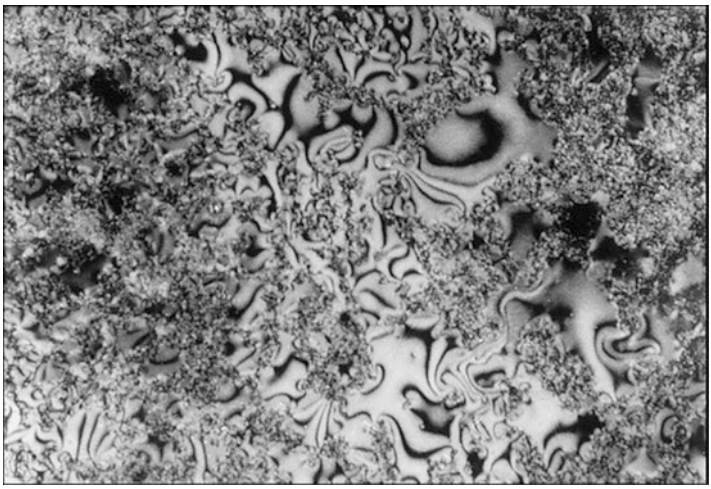

Fig. 9.2 The schlieren texture of poly[4-[(4-acryloyloxycardanyl)azo]benzoic acid]. Reproduced with permission from Saminathan and Pillai (2000). Copyright Elsevier

well as aromatic amines (Bajpai and Nivedita 1996). An aromatic aliphatic polyamide poly (p-phenylene dimeramide) [PPD] was prepared from the dimer acid and para phenylene. Lamellar LCs derived from natural sources like shea butter and jojoba oil are effective in replenishing the texture of the skin and hence widely used in the preparation of cosmetics and creams.

9.2.2 Lipid Based LCP

Amphiphilic lipids are a unique class of compounds that do not exhibit abrupt transitions from the solid to the liquid state, but do undergo 'intermediate' states, where properties of solid crystals and of liquids can be observed (Lee 1997). This so-called mesomorphic behavior can be attributed either to temperature changes, heating causes 'chain melting' which means transformation of the alkyl chains into a less ordered state owing to increased occurrence of thermodynamically unfavorable chain kinks and consequently increased chain space requirement ('thermotropic phase transition'), or changes in hydration state, leading to polar head groups bind to water and become hydrated, which increases their respective space requirements and eventually results in changes in molecular packing ('lyotropic phase change'). Egg lecithin and soya lecithin are excellent examples of this type of amphiphilic lipids that are capable of transformation into LCs and find application in parenteral drug administration. Liposomes are vesicles formed by amphiphilic phospholipid bilayers dispersed in aqueous media (Fig. 9.3). The vesicles are in fact dispersed lamellar LCs (Almgren 1980). Polymer stabilized liposomes (PSLO)

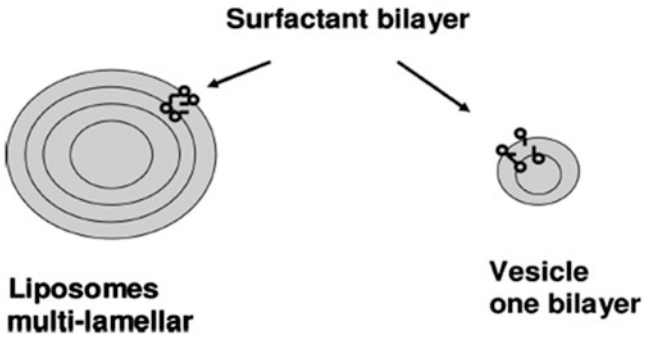

Fig. 9.3 Schematic representation of liposomes and vesicles. Reproduced with permission from Colloids and Interface Science Series, Vol. 4 Colloids in Cosmetics and Personal Care, Edited by Tharwat F. Tadros. Copyright 2008 Wiley

composed of phospholipids with polyethylene glycol chains attached to the polar head groups were prepared (Al-Bawab et al. 2005) by dissolving a blend of 1,2 dipalmitoyl-sn-glycero-3-phosphate monosodium (DPPA), 1,2 dipalmitoyl-sn-glycero-3-phosphocholine (DPPC), and 1,2 dipalmitoyl-sn-glycero-3-phosphoethanolamine N-[methoxy polyethyleneglycol] (DPPE-MPEG 5000) in polyethylene glycol followed by sonication and addition of glycerin and aqueous NaCl (Unger et al. 1992). This was followed by the addition of different amounts of orange oil to the liposome system and sonication by carefully controlling temperature within the range of 22–25 °C.

Liposomes and vesicles depicted in Fig. 9.3 are ideal systems for cosmetic applications. They offer a convenient method for solubilizing nonpolar active substances in the hydrocarbon core of the bilayer. Polar substances when intercalated in the aqueous layer of the bilayer, are capable of forming lamellar liquid crystalline phases without disrupting the stratum corneum. No facilitated transdermal transport is possible, thus eliminating skin irritation (Kim et al. 2009). Phospholipid liposomes can be used as in vitro indicators for studying skin irritation by surfactants. Glycolipids were developed by attaching a sugar group on the phenol as a hydrophilic head group and the effect of unsaturation on the gelation ability was thoroughly studied by conducting experiments with glycolipids substituted with different unsaturated chains in pure form as well as mixed form. The liquid crystalline properties of the glycolipids were studied by optical polarizing microscopy, differential scanning calorimetry (DSC) and X-ray diffraction (XRD) and the phases were identified as lamellar structure, the representative texture is shown in Fig. 9.4 (John and Vemula 2006).

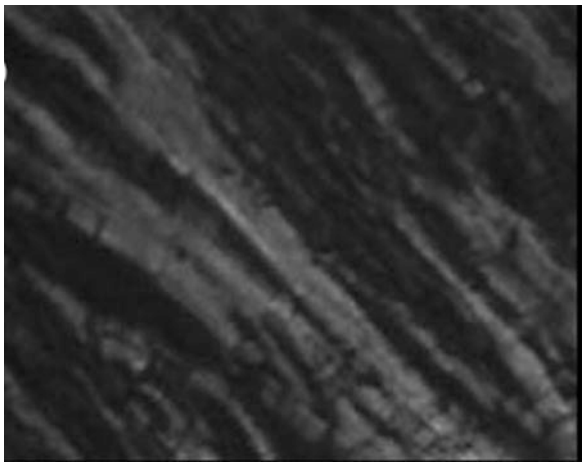

Fig. 9.4 Optical micrograph of lamellar phase of the LC derived from the glycolipid. Reproduced with permission from John and Vemula (2006). Copyright RSC

9.2.3 Cellulose Based LCPs

9.2.3.1 Nanocellulose Based LCPs

It has been known a decade back that cellulose itself is liquid crystalline in nature (Klemm et al. 2005). Due to the high aspect ratio of cellulose nano crystals (CNC), there is possibility for the formation of liquid crystalline phases. The glass transition makes it difficult to study equilibrium phases at high particle concentrations and hence the LC behavior of CNC dispersions at concentrations above 10–15 wt% is largely unexplored. It is to be believed that the glassy state is a key component in explaining the absence of observed high-order LC phases and the great variety of structural features found in films formed by drying CNC suspensions. Suppressing the glass transition or at least shifting it to a higher concentration could possibly expect a transition into a columnar LC phase in CNC suspensions. The Onsager model predicts that the required volume fraction for LC formation is inversely proportional to the rod aspect ratio and the onset concentration of liquid crystallinity is expected to decrease if the rod-like CNC is longer and thinner. Indeed, dispersions of bacterial CNCs, with lengths on the order of 1–2 mm and an aspect ratio in the range of 50–100, show nematic ordering well below 1 wt% CNC, the texture obtained under polarized microscope is given in Fig. 9.5.

Detailed investigations on the influence of the CNC counter ions on the formation of the LC phase was done by researchers and this marked an era in the chemistry of CNCs (Dong et al. 1996a, b). By adding HCl at varying concentrations to a series of CNC suspensions within the biphasic regime, such that each suspension had a constant pH of 1.61, they effectively canceled out the effect of the counter ions introduced by the cellulose nanorods. The anisotropic volume fraction curve followed a linear dependence on the CNC concentration, as expected from Onsager theory.

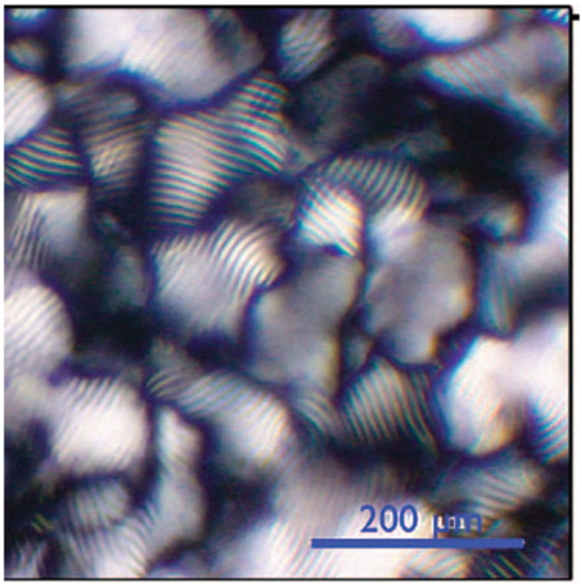

Fig. 9.5 Dispersions of bacterial CNCs showing nematic ordering well below 1 wt% CNC (Reproduced with permission from Lagerwall et al. (2014). Copyright Nature Publishing Group)

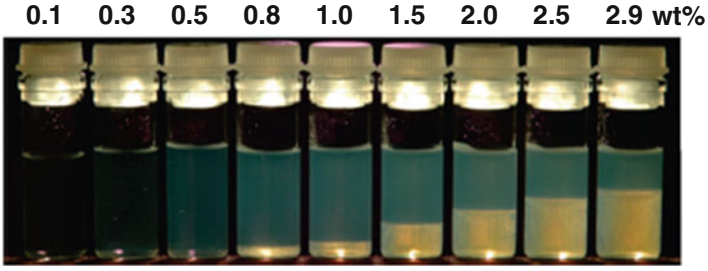

Fig. 9.6 Photograph of bacterial CNC dispersed in water at different concentrations. As the concentration increases the volume fraction of the cholesteric phase increases. Reproduced with permission from Hirai et al. 2009. Copyright ACS

Phase separation phenomena of aqueous suspensions of CNC have been studied for bacterial cellulose (BC) prepared by sulfuric acid hydrolysis (Hirai et al. 2009) and they observed an interesting and rather peculiar reversal in phase behavior in their study of bacterial CNC with added NaCl as indicated in Fig. 9.6. The shape and size distribution of BC nanocrystals in both the phases were determined by transmission electron microscopy (TEM) and atomic force microscopy (AFM). The surface charge density was determined by conductometric titration. Although the volume fraction of the cholesteric phase initially decreased with added salt, as expected, it started increasing again at concentrations greater than 0.75 mM NaCl. The entire CNC suspension was anisotropic at 2 mM NaCl, and because no stripes

indicative of a helical structure could be observed, the phase appears to have been chiral nematic with an infinite pitch (P) (Hirai et al. 2009).

The ability of CNC suspensions to form self-assembled helical structures suggests the potential of CNCs to be utilized as novel materials with attractive photonic and mechanical properties. While the CNC helix is always left-handed, reflecting the intrinsic chirality of crystalline cellulose, the value of the P can vary greatly, from less than 1 to 50 mm and beyond. The P depends on the quality of the CNC, on the concentration, on the ionic strength of the solution and may even on the temperature (Beck et al. 2013). Many aspects of helix formation are yet to be known. It is important to distinguish between the helical director modulation in liquid crystalline suspensions and helical structures found in dried films. While the former reflects equilibrium situation (provided there is sufficient equilibration time), the internal structure of a dried film is representative of the conditions prevailing within a domain when it entered the gel-like glassy state. The glass formation is a non equilibrium process that is difficult to control and there are strong variations from time to time and between different regions. Characteristic regularly spaced helix lines in an aqueous suspension with 5 wt% CNC derived by sulfuric acid hydrolysis of wood pulp is indicated in Fig. 9.7a. The distance between two lines is half the pitch (P/2), as illustrated in the schematic; hence, the equilibrated helix of this sample has a P of 13 μm. Figure 9.7b–d indicates the typical dried film of CNC (same source as above, starting concentration 4.8 wt%) with non uniform helix orientations and a strong spread in P, observed in reflection. In Fig. 9.7b, the film is illuminated with linear polarized light and observed through a crossed polarizer (analyzer). In Fig. 9.7c, d, it is illuminated with unpolarized light and observed through a l/4 phase plate followed by the analyzer, together constituting

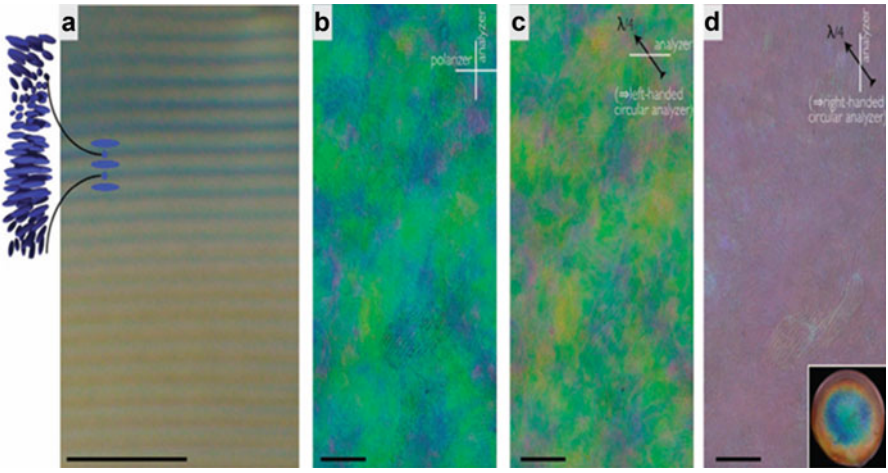

Fig. 9.7 Polarizing microscopy textural traces of CNC helix formation in the liquid crystalline (wet) state (**a**) and in solid CNC samples obtained by drying (**b–d**). *Scale bars* correspond to 50 mm (Reproduced with permission from Lagerwall et al. (2014). Copyright Nature Publishing group)

an analyzer for left- Fig. 9.7c and right-handed Fig. 9.7d circular polarization, respectively. The inset in Fig. 9.7d shows the iridescence from a macroscopic, dried CNC film on a circular glass substrate (25 mm in diameter) against a black background, viewed at a slight angle (Lagerwall et al. 2014).

Sulphuric acid when used as a hydrolyzing agent chemically reacts with the surface hydroxyl groups of CNCs to yield negatively charged (surface) sulfate groups that promote a perfectly uniform dispersion of the whiskers in water via electrostatic repulsions (Revol et al. 1992). The removal of the water phase leads to a situation in which the CNCs adopt configurations that minimize the existing electrostatic interactions. It is noteworthy that (homogeneous) concentrated suspensions self-organize into brilliant liquid crystalline arrangements, exactly similar to what occurs in non-flocculating suspensions of other rod-like particles, such as poly(tetrafluoroethylene) whiskers (Folda et al. 1998), tobacco mosaic viruses (TMV) (Oster 1950), DNA fragments etc.

The chiral nematic structure can be preserved after complete water evaporation to provide iridescent films of CNCs. These solid films, in addition to allowing fundamental studies of their striking behavior, have numerous potential applications such as coating materials for decorative materials and security papers (because the optical properties cannot be reproduced by printing or photocopying) (Revol et al. 1995). An investigation into these systems reveals that CNCs are randomly oriented in the dilute regime (isotropic phase). A nematic liquid crystalline alignment is adopted when the CNC concentration increases because these tactoids coalesce to form an anisotropic phase, which is characterized by a unidirectional self-orientation of the Cellulose nano rods. When the suspension of CNCs reaches a critical concentration, it forms a chiral nematic ordered phase displaying lines that are the signature of cholesteric LCs. Various factors such as size, shape, dispersity, charge, ionic strength of the solution (electrolyte) (Fleming et al. 2001), and external stimuli can affect the liquid crystallinity, p, domain size, ordering, and other properties (Moon et al. 2011). Films with uniform nanorod alignment achieved by shearing were studied in detail. The nature and density of the charges on the surface of CNCs have also been reported to affect the formation of the chiral nematic phase. By using post-sulfated HCl-hydrolyzed CNCs, which have sulfur content approximately one-third less than directly H_2SO_4-hydrolyzed CNCs, it has given distinctly different behaviors. Indeed, post-sulfonated suspensions formed a birefringent glassy phase having a crosshatch pattern (Fig. 9.8) rather than a fingerprint pattern indicative of chiral nematic phases and are typical of directly sulfated CNCs (Araki et al. 2000).

The study of alignment of a liquid crystalline CNC suspension under shear flow with varying shear rates using X-rays was conducted by Ebeling et al. (1999) and found that the suspensions exhibited quite complex behavior, with results that are very much dependent on the shear rate. When the films prepared using different starting concentrations were dried under continuous shear flow, dried films gave interesting internal structures.

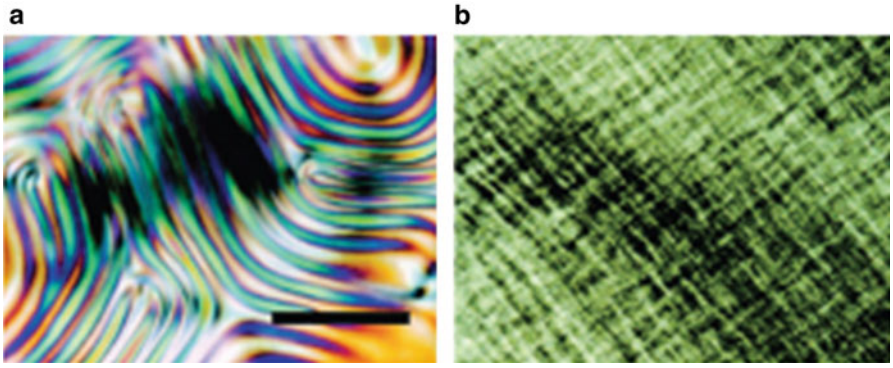

Fig. 9.8 Polarized-light micrographs of CNC suspensions: (**a**) fingerprint pattern in the chiral nematic phase of the directly H_2SO_4-hydrolyzed suspension (initial solid content, 5.4 %); (**b**) crosshatch pattern of post sulfated suspension (solid content, 7.1 %). Reprinted with permission from Araki et al. (2000). Copyright 2000 American Chemical Society

9.2.3.2 Cellulose Derived LCPs

Cellulose constitutes the most abundant renewable polymer as it is derived from plants. As mentioned earlier, cellulose as such and a large number of its derivatives form liquid crystalline phases either lyotropic or thermotropic. Here we discuss the mesogenic properties of cellulose and its derivatives. Rogers et al. suggested an environmentally benign method for preparing cellulose solutions containing up to 25 wt% cellulose using ionic liquids. Compositions between 5 and 10 wt% cellulose were prepared using 1-butyl-3-methylimidazolium chloride ([C4mim]Cl) as the solvent. Viscous solutions of cellulose with concentrations above 10 wt% in [C4mim]Cl, yielded liquid crystalline materials and exhibited optical anisotropic and birefringence when viewed under polarized microscope. High-strength materials that conserve anisotropy in the solid phase are especially desirable, because of the enhanced mechanical properties they may possess (Swatloski et al. 2002).

It is noteworthy that, most of the cellulose derivatives exhibit cholesteric LC phases in solutions within certain concentration regions (lyotropic) or in the bulk within certain temperature regions (thermotropic). The physical packing (chiral arrangement) schemes of stiff cellulose chains are considered to be playing important roles in inducing the formation of cholesteric LC phases. In particular, when the flexible side chains are connected onto the cellulose backbones, the resulting hairy-rod cellulose polymers start forming these cholesteric LC phases. It is considered that the attachment of flexible side chains onto the rigid cellulose molecules facilitate the orientational order of the semi-rigid hairy-rod backbones (Tseng et al. 1982; Hou et al. 2000) is considered as one of the important approaches towards obtaining cellulose derivatives with cholesteric LC phase transitions. Among the cellulose derivatives, hydroxyl propyl cellulose (HPC) derivatives are

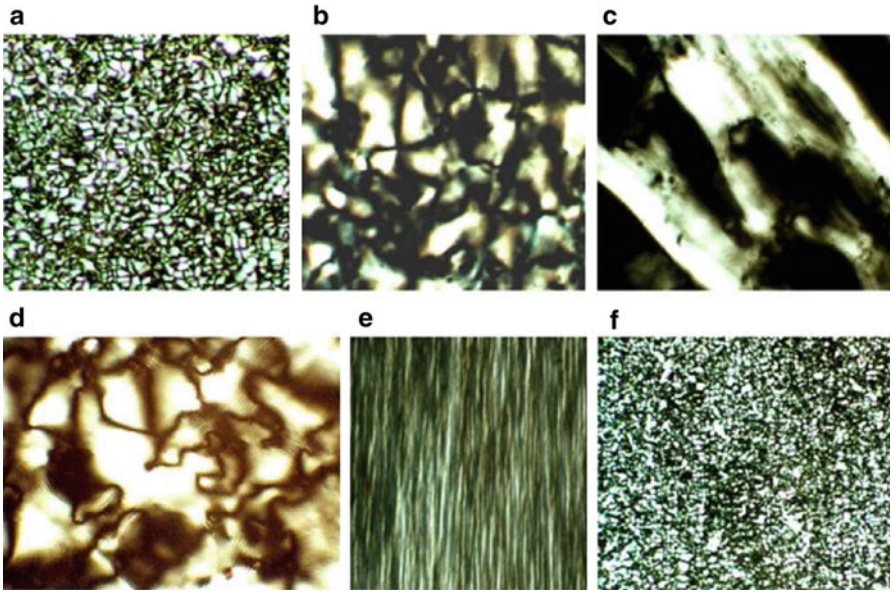

Fig. 9.9 Polarized light microscopic graphs of CnPC texture (at 25 °C): (**a**) C3PC 150°; (**b**) C6PC 750°; (**c**) C7PC 750°; (**d**) C10PC 375°; (**e**) C6PC 375°, *arrow* directs shear force direction; (**f**) C2PC annealed at 150 °C for 20 min, 150°. Reproduced with permission from Huang (2007) Copyright Elsevier

of specific interest because they can form either cholesteric lyotropic or thermotropic LC phases (Hou et al. 2000). LC behaviour of derivatives of HPC (CnPC) with different side chain lengths are studied (Huang 2007) as an attempt towards the systematic understanding of the side chain effect on the formation of thermotropic cholesteric LC phases and phase transitions as well as their unique selectivity for color reflections and the pitch distance in the cholesteric LC phases. The representative schlieren textures obtained for polymers C3PC, C4PC, C5PC, and C6PC at room temperature (Figs. 9.9a, b) represents the formation of the low-ordered LC phases. Under a mechanical shear force at elevated temperature, all of the CnPCs present typical banded textures of low-ordered LC phases (Fig. 9.9e for C6PC). At 150 °C, a Schlieren texture of C2PC retains before the isotropic melt (Fig. 9.9f). In this study it was found that the increase in the number of methylene units of side chain narrowed the thermotropic phase transition window and the layer spacing increases of the cholesteric LCs increases linearly with increase in the methylene units in the side chains, and the corresponding pitch distance of the cholesteric LC phases are strongly dependent on the number of methylene units in the side chains, and the twisting angle and the layer number in the helical structure are also depended on the length of methylene units in the side chains in this polymer series.

A particularly interesting property of the cellulose derivatives is that, based on different chemical structures, the materials can reflect light at a specific light

wavelength in a specific temperature region. Cellulose derivative with such property was prepared from HPC as follows. 5.0 g of HPC (corresponding to 41.71 mM of hydroxyl groups) was added to 30 mL acetone under a dry nitrogen atmosphere and was dissolved by heating the solution. Then 15.1 mL (125.13 mM) valeric acid chloride was swiftly added to the solution of HPC by using a syringe. After 2 h of reflux, the reaction mixture was poured into 200 mL of distilled water. After removing the liquid phase, a cream-colored, sticky material was obtained and then dissolved in 80 mL acetone and precipitated by adding 5 mL of water to the solution. The pasty product was liberated from the acetone/water by decantation. The second solution precipitation was repeatedly done and the product was obtained by drying at 60 °C for 48 h.

9.2.4 LCPs of Biological Origin

It is interesting to note that many of the biological structures exhibit liquid-crystal behavior, for instance glycolipids, polypeptides, DNA etc. exhibit various LC phases. The concentrated protein solution extruded by a spider to form silk is known to be in LC phase and the precise ordering of molecules in LC phases is thought to be critical to its renowned strength. The in vivo DNA concentrations are also thought to be in the LC phase. Likewise many such biological structures are proposed to be in LC phase and the LC phase may have a crucial role in their exceptional properties. It can be seen that all the systems mentioned are capable of forming self assembled structures.

9.2.4.1 Protein Based LCPs

Spider silk is made of β-crystallites enriched with polyalanine repeats of the protein within a matrix of the less ordered glycine-rich segments (Rathore and Sogah 2001). The polyalanine segments form transverse lamellae within oriented nanofibrils, when extruded from the duct and exhibit nematic ordering (Knight and Vollrath 2002). However, mechanically drawn fibres do not show the same texture, instead show a banded texture, indicating a periodic variation in director orientation, in contrast to fibres extruded from silk glands (Kerkam et al. 1991). Spider dragline silk is considered as a LC elastomer due to its structural and elastomeric properties. The nematic phase of spider and silkworm fibroin observed in aqueous solutions is thought to serve as an intermediate state in the in vivo processing route of fibril orientation. Similarly, fibrillisation of the silk-moth chorion protein (found in the eggshell) is also considered to precede from LC phase nuclei, in particular amyloid spherulites. Silkworm (Bombyx mori) silk is rich in GAGAGS repeats. LC phases have been observed for block copolymers comprising PEG (polymer) conjugated to the Bombyx mori-silk inspired GAGA domain and for PEG/peptide multiblocks containing poly(alanine) repeats, based on the Nephila clavipes spider

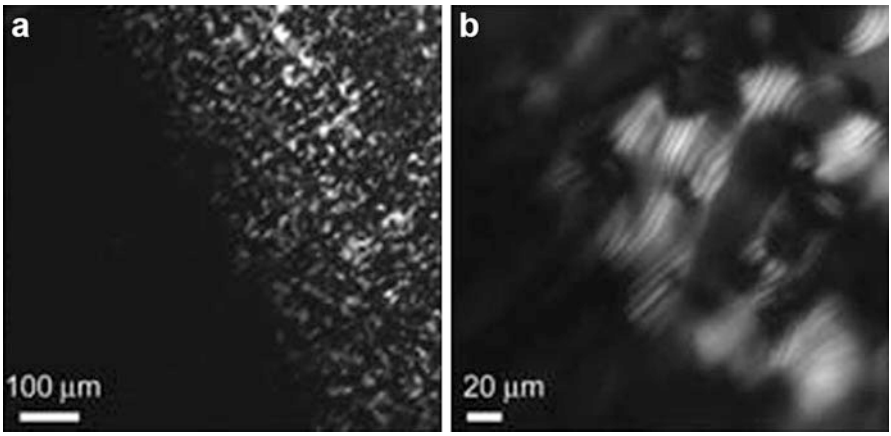

Fig. 9.10 Polarized optical microscopy images of (**a**) I/N interface in a type II collagen solution at 5 mg mL^{-1} in 0.5 Macetic acid, after drying, (**b**) same region at higher magnification showing typical fingerprint texture. Reproduced with permission from Belamie et al. (2006) Copyright IOP science

silk structure. Poly g-benzyl-L-glutamate (PBLG), adopts an α-helical conformation in organic solvents and in the melt when the chain is sufficiently long (Elliott and Ambrose 1950) and forms chiral nematic and columnar phases in organic solvents such as m-cresol or pyridine (Luzzati et al. 1961; Robinson 1966).

The most significant helical bio macromolecule which forms LC phase, other than the DNA, is the collagen. Collagen, the most abundant protein in higher animals gives the supporting frame in which organs and tissues are shaped, and is also responsible for the firmness, elasticity and integrity of structures and hydration of the body. Type I collagen plays vital role in tissues such as tendon, skin, bone and cornea and the Type I collagen monomers can form nematic, precholesteric and cholesteric phases in dilute acid solution (Giraud-Guille 1992) (Fig. 9.10). Collagen possesses high tensile strength and good elasticity, and hence is considered as a biological LC elastomer. Liquid crystallinity of collagen is observed under conditions close to that of found in tissues (50–200 mg mL^{-1}) (Giraud-Guille et al. 2008) Therefore, it can be thought that self-assembly of mesophases play a role in the mechanism of ordering of collagen in bones, fish scales and cornea as well as of chitin fibres from arthropods (Belamie et al. 2006).

Another protein structure which exhibit self assembly and LC phase is the neuronal proteins. The three filamentous proteins: filamentous actin (Safinya 2006; Hirst et al 2005), microtubules, (Choi et al. 2009; Safinya et al. 2011) and neurofilaments (Jones and Safinya 2008; Beck et al. 2010a, b; Deek et al. 2013) constitute the major protein fraction in the cytoskeleton of neurons. The lengths of rigid microtubules are in the order of millimeters, of semi-flexible filamentous actin is about one micron and of flexible neurofilaments is around 100–150 nm. The large difference in their rigidity leads to quite different hierarchical self-assembled structures for these different filamentous systems. The 3D bundles of MTs

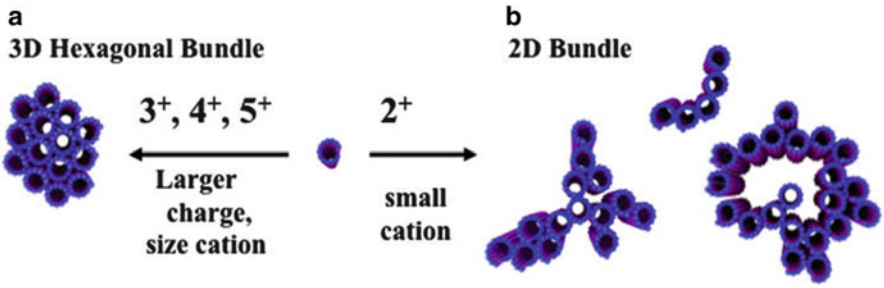

Fig. 9.11 Schematic of higher-order-assembly of microtubules in the presence of multivalent counterions. (**a**) Trivalent (spermidine $[H_3N^+\text{-}(CH_2)_3\text{-}NH_2^+\text{-}(CH_2)_4\text{-}NH_3^+]$ and lysine3), tetravalent (spermine $[H_3N^+\text{-}(CH_2)_3\text{-}NH_2^+\text{-}(CH_2)_4\text{-}NH_2^+\text{-}(CH_2)_3\text{-}NH_3^+]$ and lysine4), and pentavalent (lysine5) cations lead to the formation of 3D bundles with hexagonal in-plane symmetry. (**b**) Divalent cations $[(Ba^{2+}, Ca^{2+}, Sr^{2+})]$ lead to the sheet-like 2D bundles with linear, branched, and loop morphologies. Reprinted with permission from Needleman et al. (2004). Copyright 2004, National Academy of Sciences, U.S.A

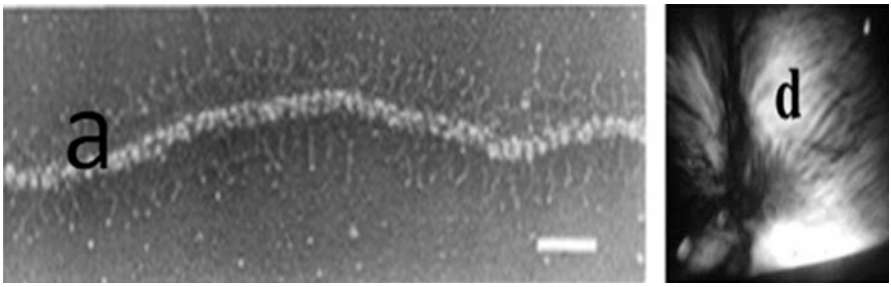

Fig. 9.12 (**a**) Electron micrograph of a mature neurofilament (glycerol sprayed/low-angle rotary metal shadowed on freshly cleaved mica). The side arms are clearly visible. The bar is 100 nm. (**b**) A reconstituted NF mixture forming a strongly birefringent hydrogel viewed between crossed polarizers shows the presence of nematic-like liquid crystalline texture, (**a**) is reproduced with permission from Herrmann, H.; Kreplak, L.; Aebi, U. Methods in Cell Biology. Omary, MB.; Pierre, AC., editors. Vol. 78. Academic Press; Waltham, MA: 2004. p. 3–24, (**b**) is reproduced with permission from Needleman DJ, Jones JB, Raviv U, Ojeda-Lopez MA, Miller HP, Li Y, Wilson L, Safinya CR. Supramolecular assembly of biological molecules purified from bovine nerve cells: from microtubule bundles and necklaces to neurofilament networks. J Phys: Condens Matter. 2005; 17:S3225–S3230

(Fig. 9.11), with in-plane hexagonal symmetry observed by small-angle-X-ray-scattering (SAXS) studies, are similar to that of freely suspended columnar phases of discotic LCs (Van Winkle and Clark 1982; Safinya et al. 1984).

Neurofilaments consist of three different molecular weight polypeptide subunits (Fig. 9.12a, labeled NF-L (L = Low, 60 kDa); NF-M (M = Medium, 100 kDa); and NF-H (H = High, 115 kDa)). Among the fractions only NF-L assemble in the absence of the other subunits and form stable filaments and both the NF-M or NF-H subunits require the presence of NF-L to form filaments. In buffer mimicking

physiological conditions, purified and re-assembled NFs may form an Onsager-like nematic LC gel phase, and tend to spontaneously assemble to form a 10 nm thick filamentous protein with highly charged C-terminal sidearms, which extend away from the filament (Fig. 9.12a) (Ching and Liem 1993; Fuchs and Cleveland 1998). PPLM observations revealed images of a nematic hydrogel (Fig. 9.12d), with long-range orientational order associated with the filamentous network (Beck et al. 2010a, b; Needleman et al. 2005; Jones and Safinya 2008; Hesse et al. 2008). The neurofilament nematic gel phase, made in vitro was found to be a thermodynamically stable phase and was found that the stability is dependent on the salt concentration. As a function of decreasing salt concentrations, the nematic gel phase undergoes reversible transitions to an isotropic gel followed by a new re-entrant LC gel phase (Deek et al. 2013).

Similarly, NF from the principal cytoskeletal constituent of myelinated axons vertebrates have an assembled filament structure with protruding flexible C-terminus side arms and exhibit LC phase (Fig. 9.13). The LC gel networks of the neurofilament assemblies assumed to play a key role in the mechanical stability of neuronal processes and in long myelinated neuronal axons, the neurofilaments form an aligned nematic liquid-crystal gel with an open-network structure and acts as a structural scaffold. The side arms play a critical role in modulating the forces

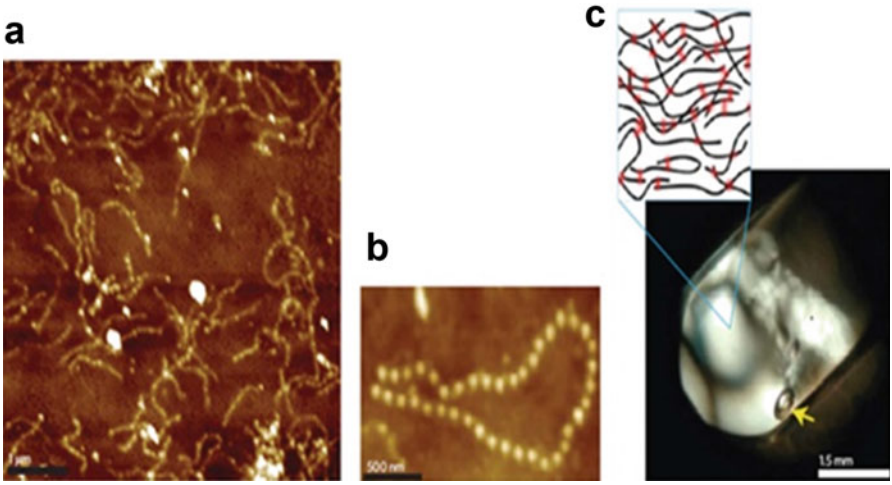

Fig. 9.13 Hierarchical neurofilament self-assembly. (**a**, **b**) AFM images that show a necklace structure and a preferred parallel configuration even at a low protein concentration. (**c**) Cross-polarized microscopy image of a neurofilament network in a quartz capillary. Cross-polarized microscopy image of a neurofilament network in a quartz capillary. The nematic domain boundaries are a clear indication of the extended length scale of the ordered phase. The non-spherical bubble (*yellow arrow*) reveals the yield stress resisting surface tension, as expected for a gel. The inset illustrates the possible configurations and microscopic interactions, such as physical entanglement or intrafilament and interfilament interactions, leading to the nematic order. Reproduced with permission from Roy Beck et al. (2009). Copyright Nature Publishing group

between neurofilaments in their isotropic and liquid-crystal gel phases (Beck et al. 2009). The alignment of the neurofilament hydrogel is established clearly with the help of cross-polarized microscopy as shown in the Fig. 9.13.

DNA, a biopolymer, with its structure and functions based on self assembly, exhibiting liquid crystalline properties is not surprising. Michael W. Davidson and coworkers in 1998 showed that DNA exists in LC phases at certain DNA concentrations, thus exhibiting lyotropic LC behaviour. DNA has found to form at least three distinct liquid crystalline phases at concentrations comparable to those in vivo: a weakly birefringent, dynamic 'precholesteric' mesophase with microscopic textures intermediate between those of a nematic and a true cholesteric phase, a second mesophase which is a strongly birefringent, well-ordered cholesteric phase and at highest concentrations, a third phase which resembles that of smectic phases of thermotropic LCs (Davidson et al. 1998). Crystalline solutions of DNA at concentrations of 130–170 mg DNA mL^{-1} at room temperature, become fully liquid crystalline at higher concentrations. Phase transition boundaries were in good agreement with predicted rigid rod behaviour when DNA was treated as a scaled rod with an effective radius of 21.5 Å at this ionic strength (Fig. 9.14).

It is well known that multivalent cations can condense DNA to LC phases, for instance, polyamines condense DNA to LC phases, cationic liposomes form a lamellar structure with DNA. Synchrotron X-ray scattering studies of cationic liposome (CL-DNA) complexes have led to the discovery of distinct structures such as a multilamellar phase with DNA layers sandwiched between cationic bilayer membranes (L_α^C), (Rädler et al. 1997) and an inverted hexagonal structure with DNA encapsulated within cationic lipid monolayer tubes (Koltover et al. 1998). The lamellar CL-DNA complex is a "hybrid" phase of matter with DNA chains layered between lipid bilayers (Fig. 9.15), forming a 3D smectic phase (Ewert et al. 2006; Zidovska et al. 2009).

9.2.4.2 Chitin and Chitosan Based LCP

Chitin, a long-chain polymer, found in the exoskeleton of arthropods such as crustacean and insects can be processed by acid hydrolysis to produce rod-like nanoparticles which can form a chiral nematic phase at sufficiently high volume fraction, depending on pH and ionic strength. Hydrolysis of α-chitin, obtained from crab shells generates rod-like crystallites, with a width and length of 6–8 and 100–200 nm, respectively, Figs. 9.16a, b show the representative textures. It has been proposed that the chiral nematic phase act as a template for the helicoidal arrangement of chitin microfilaments. Iridescent colouring of certain beetle wings (Fig. 9.18) is proposed to be due to the helicoidal stacking of fibrous chitin layers, and it is possible that LC phases may be acting as precursors to the stacking structure.

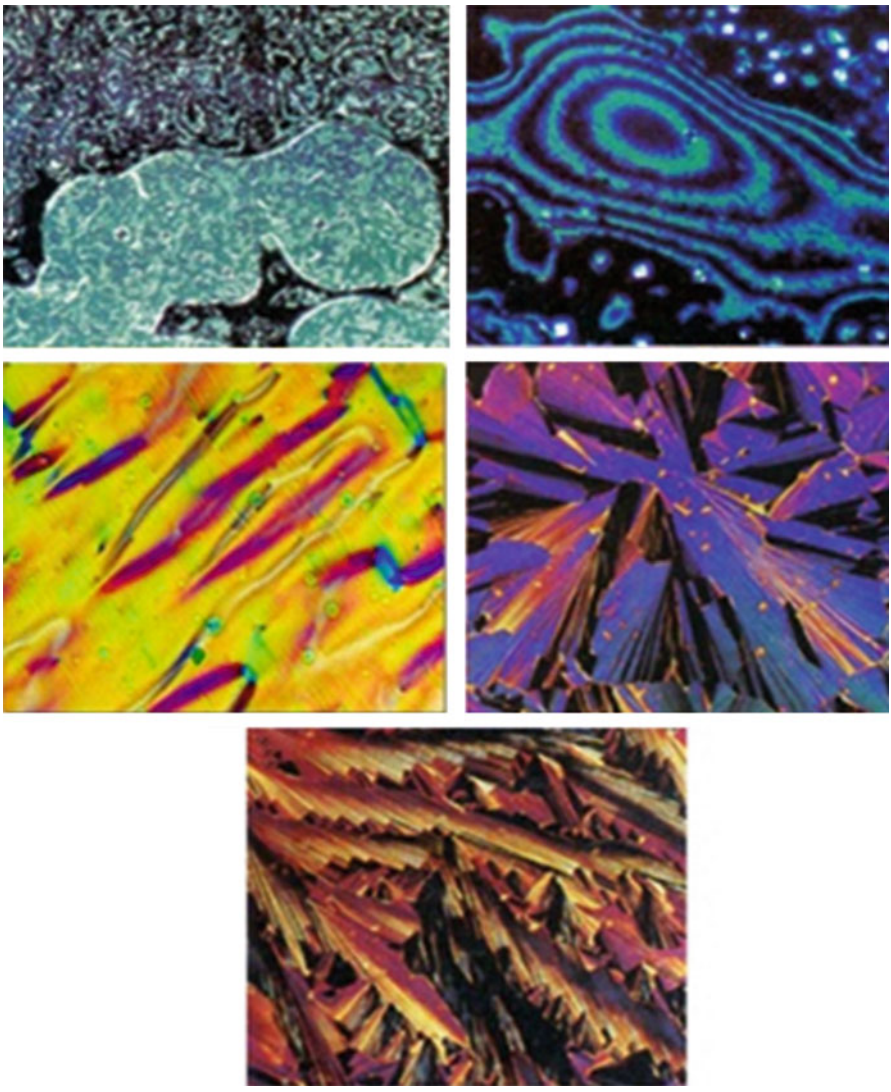

Fig. 9.14 (*Top* to *bottom*, anti clockwise): Low magnification views illustrating sharp transition zones between precholesteric and cholesteric domains, Weakly birefringent, diffuse ring texture of 'precholesteric' phase, Highly birefringent, fringe or chevron texture of magnetically aligned cholesteric phase of DNA, Focal-conic-fan texture of smectic-like phase, Pleated ribbon' texture of most concentrated smectic-like phase near open end of coverslip (Reproduced with permission from Teresa et al. (1998) Copyright Nature Publishing group)

Chitosan is yet another biologically derived polymer which can be converted to liquid crystalline material and several works have reported the preparation of LCs from chitosan and its derivatives. Similarly Sakurai and coworkers reported the preparation of thin films and fibres from 38 % chitosan/formic acid solution.

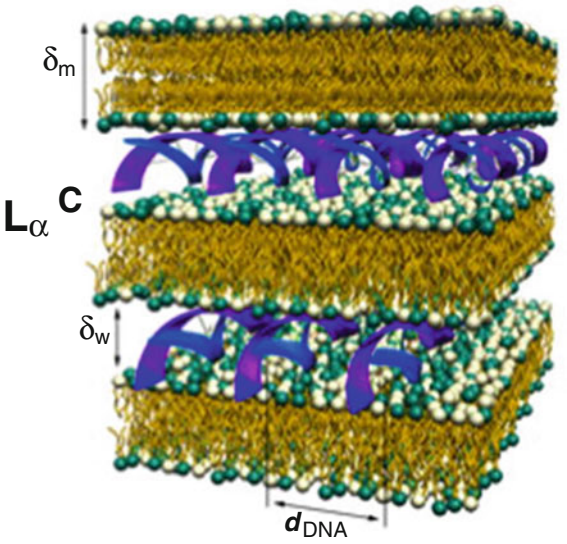

Fig. 9.15 The structure of three distinct cationic liposome CL-DNA complexes determined by synchrotron small-angle X-ray scattering. Reproduced with permission from Safinya et al. (2013). Copyright Taylor and Francis

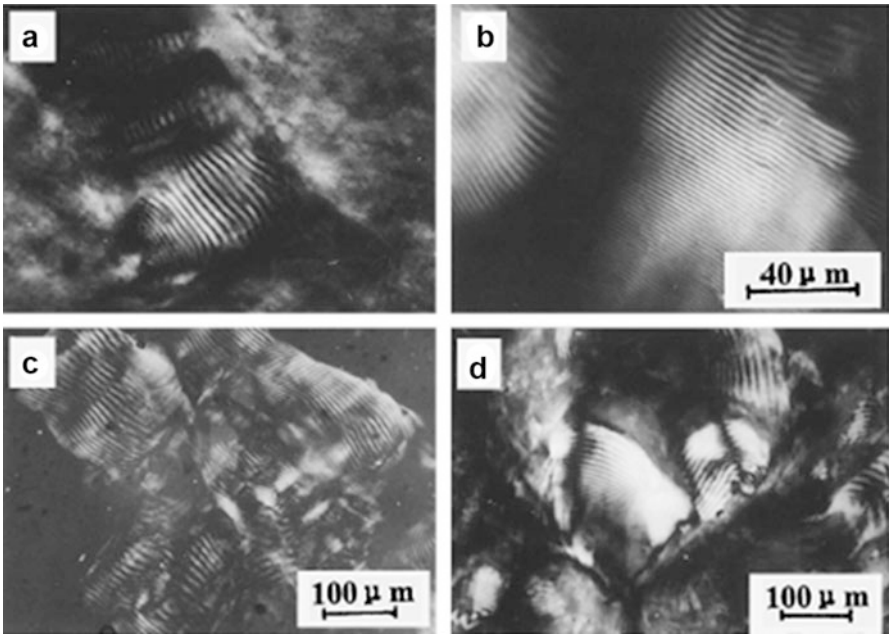

Fig. 9.16 (**a**) Photomicrographs of cholesteric LC texture of HPCS solutions (**b**) 15 wt% HPCS1/DCA solution; (**c**) 18 wt% HPCS6 aqueous solution; (**d**) HPCS7 wet product. Reproduced with permission from Yanming Dong et al. 2001. Copyright Elsevier

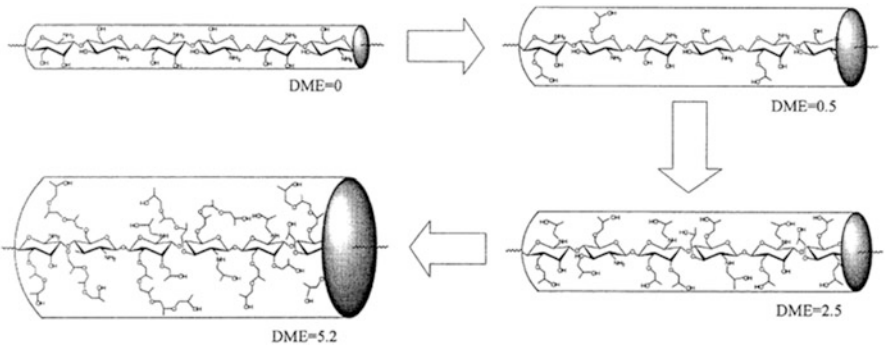

Fig. 9.17 Schematic illustration of the increase of HPCS molecular diameter with enhancement of DME. Reproduced with permission from Yanming Dong et al. (2001). Copyright Elsevier

Hydroxypropyl chitosan with different degree of molar etherification were prepared and studied by Yanming Dong and his coworkers (Dong et al. 2001). It was found that the critical concentration for formation of the lyotropic LC is very high in the case of chitosan due to the breaking of hydrogen bonds in chitosan. As a result a small substitution in chitosan thus results in a large increase in critical concentration. It can be shown that the diameter of the macromolecules increases with the increase of DME as shown in the Fig. 9.17. The chitosan derivatives were prepared as follows: an alkaline chitosan solution is prepared by dissolving chitosan in NaOH solution and stored at −18 °C overnight before use. An excess of poly ethylene oxide is added to the defrozen alkali chitosan and stirred, refluxed and cooled and subsequently neutralized using HCl and washed with water and acetone alternately and dried in vacuum. The as prepared chitosan derivatives analysed in different solvents like water, formic acid and dichloroacetic acid were found to exhibit cholesteric liquid crystalline phase.

9.3 Characterization of Liquid Crystals

Several methods are used for the characterization of the liquid crystalline phase, some of the common techniques are DSC, PLM, XRD etc. Some of the characterization techniques of LCs are explained using examples.

9.3.1 Differential Scanning Calorimetry

DSC is an important tool to determine transition temperatures and to distinguish the different phases. The lamellar liquid crystalline structure of para phenylene dimeramide (PPD) synthesized using castor oil as precursor was confirmed using

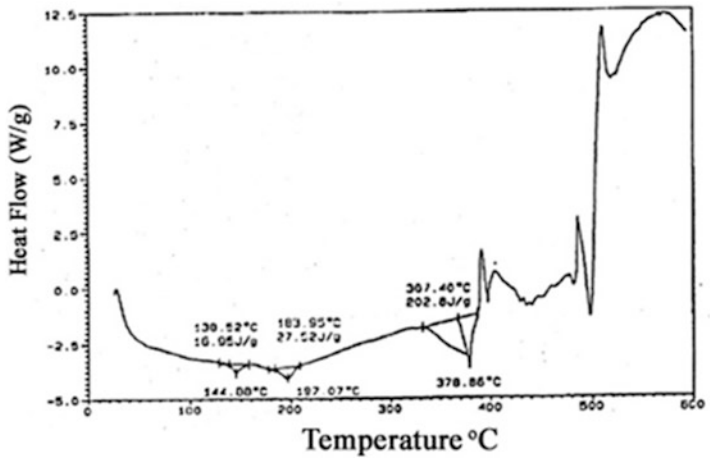

Fig. 9.18 DSC analysis of PPD (Reproduced with permission from Khare et al. 2013. Copyright KROS publisher)

this technique. The three endothermic curves in the DSC analysis (Fig. 9.18) indicate the presence of intermediate transitions/phases in the substance. From the PLM studies the peaks are assigned to the following phases: the first endotherm corresponds to the crystal to smectic phase transition, the second endotherm, smectic to nematic phase transition, and the third endotherm highlights the phase transition from nematic to isotropization.

DSC can also be used to study the dependence of the phase transitions on the structure of the compound. Figure 9.19 shows a set of DSC cooling diagrams for a series of aliphatic esters of 2-hydroxy propyl cellulose (CnPCs). It is evident that by increasing the length of the side chains, both the LC phase to the isotropic melt, ΔH_i and the LC phase to the isotropic melt transition temperatures T_i decreases. This shows that not only the backbones but also the side chains are involved in these transitions; the transitions are dependent on the length of the side chains significantly. When cooled further, it leads to a vitrification of the materials (as shown in Fig. 9.19). The glass transition temperature (T_g) of CnPC also decreases as the number of methylene units in the side chains increases. It is clear that the methylene units in the side chains not only serve as "diluents" but also involve in these phase transitions by providing contributions to the enthalpy of the isotropic melt to LC phase transitions. Moreover the methylene units of CnPC affect the T_g while the T_g drops with the increase in the length of the methylene units. Thus from the DSC it is evident that not only the backbones but also the side chains influence the formation of the LC phases and phase transitions.

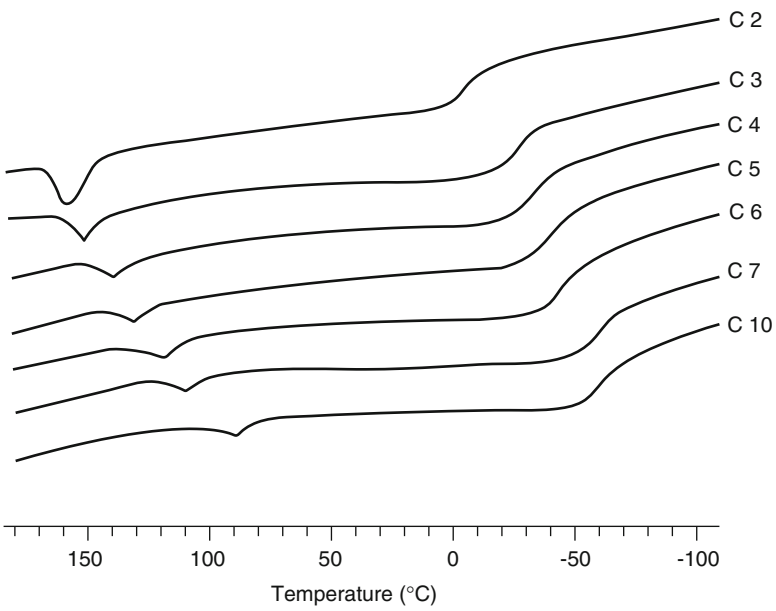

Fig. 9.19 DSC cooling curves of CnPC recorded at 15 K/min and normalized per gram of material. Reproduced with permission from Huang Polymer (2007). Copyright Elsevier

9.3.2 Polarized Light Microscopy

PLM is a widely used technique to study and identify the phases exhibited by LCs. A thin layer of a LC is placed in between two cover glass plates and viewed through a PLM under temperature or proper conditions depending on the type of LC phase, various textures can be observed. Beautiful kaleidoscopic images called textures are seen due to the interference between light waves passing through the specimen, which is already heavily given throughout the chapter.

The formation and growth of LCs in nanocellulose was observed by means of laser diffraction. The laser beam produces a diffraction pattern and the central spot of the ring grows into a steady circular ring showing the growth of LCs and their organization into larger assemblies which is confirmed by the appearance of concentric rings after some time. Optical microscopy is an important tool for the study of the structure of lamellar LCs. Many microscopic techniques like SEM, TEM and AFM are commonly used. Chiral nematic phases have been observed for concentrated solutions and melts of many cellulose derivatives (Gray 1995). Both left and right-handed solutions, melts and films have been observed for cellulose derivatives, but to date only left-handed helicoids have been observed for CNC suspensions and films. The assignment of handedness was based on TEM images of oblique microtomed sections of films cast from aqueous suspensions of CNCs, following the interpretation of the arcing observed in

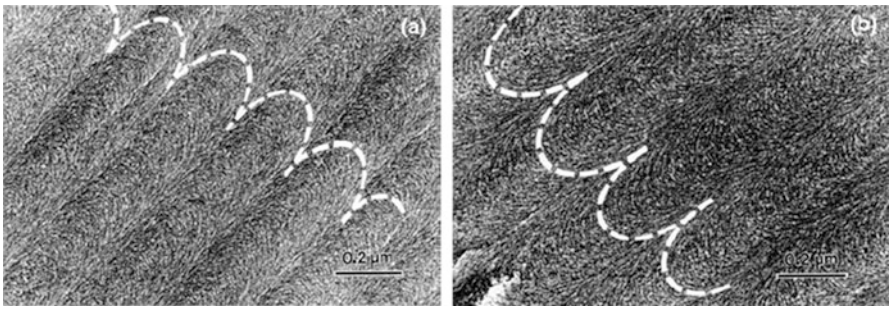

Fig. 9.20 Arcing observed in TEM images of thin oblique cross-sections through a planar chiral nematic film of wood CNCs cast from aqueous suspension on a Teflon substrate. The sections were cut at angles such that the top left-hand corner of the image was tilted (**a**) towards and (**b**) away from the observer (Giasson 1995) (Reproduced with permission from Dissertation, McGill University, Chap. 5, p 167)

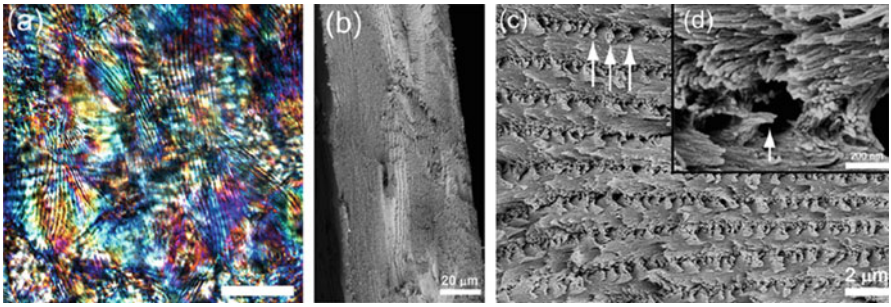

Fig. 9.21 (**a**) Optical microscope image (*crossed polars*) of the bulk CNC film (*scale bar* 40 lm), (**b**–**d**) SEM images of a fracture surface across the film (Majoinen et al. 2012) (Reproduced with permission from Springer)

natural composites by Bouligand (2008). Arcing observed in TEM images of thin oblique cross-sections through a planar chiral nematic film of wood CNCs cast from aqueous suspension on a Teflon substrate is shown in Fig. 9.20 (Giasson 1995).

When the cast CNC film is viewed in transmission between crossed polars in an optical microscope (Fig. 9.21a) the film shows the usual multi domain structure, where the direction of the chiral nematic axis changes with the location in the film. The shortest distance between the lines is P/2. The fan-like appearance found in the SEM in Fig. 9.10d corresponds to the cross-section of a left-handed helicoidal arrangement of CNC, with the axis of the helicoid from top to bottom of the image.

The LC properties exhibited by spherical nano cellulose suspensions were reported for the first time by Neng et al. and the liquid crystalline textures were carefully observed using PLM (Wang et al. 2008). The formation of nano crystals from spherical nanoparticles is thermodynamically unfavorable as per

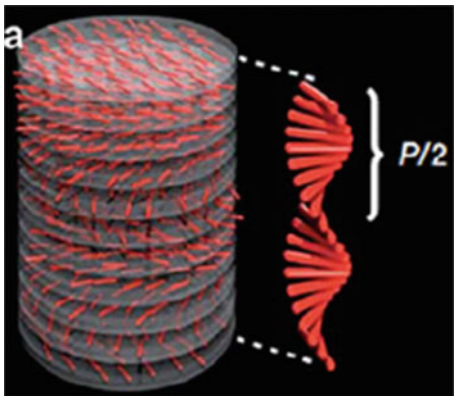

Fig. 9.22 Schematic representation of chiral nematic ordering present in nanocrystalline phase (Reproduced with permission from Shopsowitz et al. (2010a, b). Copyright ACS 2010)

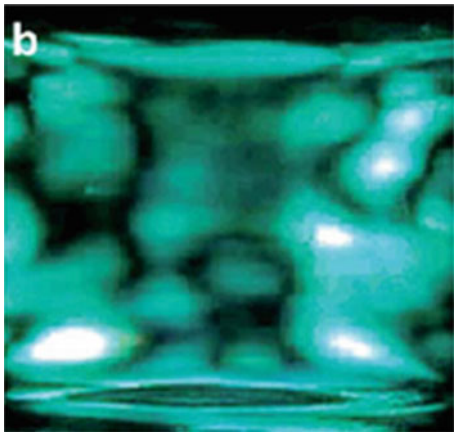

Fig. 9.23 Photograph of an aqueos suspension of tunicin whiskers as observed through cross nicols. Reproduced with permission from Azizi Samir et al. (2005). Copyright ACS 2005

Onsager's theory (Onsager 1949) whereas the LCs of rod like particles are more thermodynamically stable because of the gaining of translational entropy that overrides the loss of orientation entropy due to particle alignment (Jana 2004). The importance of cellulose lies in the fact that cellulose crystallites have a helical twist along the main axis, which can induce crystal suspensions to attain a helical twist normal to the main axis of the rod, and thus organize into a chiral nematic phase or cholesteric phase of stacked planes aligned along a perpendicular axis as shown in Fig. 9.22 (Shopsowitz et al. 2010a, b; Dong et al. 1996a, b).

This type of alignment can result in optical band gaps leading to the macroscopic birefringence of individual domains, which can be seen through crossed polarizers as the Schlieren texture as shown in Fig. 9.23 which depicts the photograph of aqueous suspension of tunicin whiskers as observed between cross nicols.

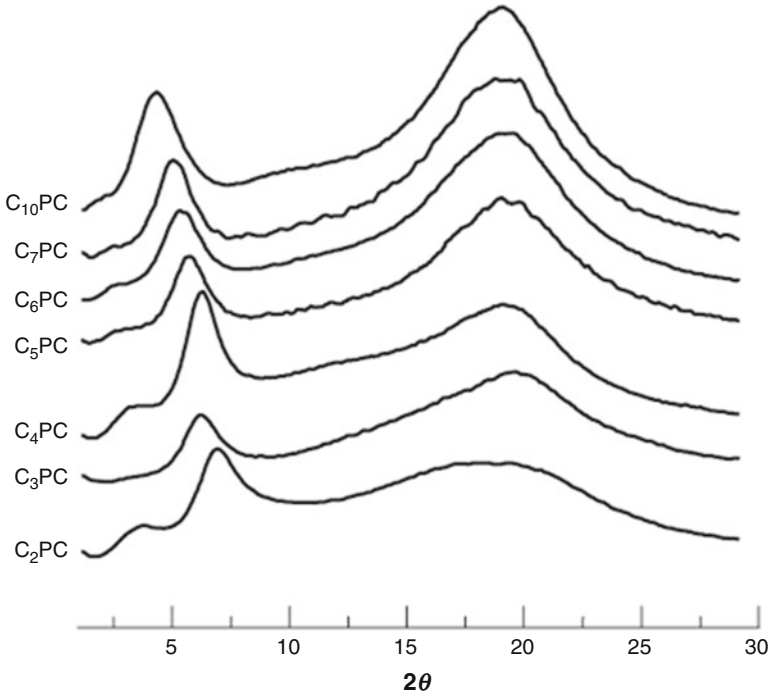

Fig. 9.24 1D WAXD powder diagram: CnPC bulk at room temperature on a glass slide in a reflection mode. Reproduced with permission from Huang (2007). Reproduced with permission from Elsevier

9.3.3 X-ray Diffraction Technique

The chain packing scheme of the thermotropic LC phase in CnPCs deduced based on wide angle XRD structural characterization technique (Fig. 9.24) displayed an intense diffraction peak in the low 2θ angle region between 3° and 8°. Furthermore, with increasing the number of methylene units, the d-spacing of the diffraction peak increases from 1.20 nm in C2PC to 1.37 nm in C5PC to 1.86 nm. These diffraction peaks represent the existence of short range or quasi-long-range positional order.

9.4 Applications of Liquid Crystals

LCs are well known for their display applications due to its light modulating properties and is been widely applied world over as display materials in computer monitors, flat panel displays, electronic display materials such as television, video etc. because of their energy efficiency and clarity compared to the conventional displays. These optical display films have uniform optical properties across the

surface area. For applications such as patterned polarization rotators for stereoscopic displays, polarization sensitive gratings, reflective colour filters and patterned polarizers, it is useful to locally tailor the optical properties of displays, adding chiral molecules to LCs, to control the twisting sense and the rotation angle, provides a method to prepare such films. Recently, new technologies have become available for the realization of such structured films. For instance, cholesteric liquid crystalline phases, the chiral nematic phases are well-known for their ability to rotate and reflect light. The wavelength of maximum reflection (λ) and the width of the band depend on the P of the cholesteric LC phase and the refractive indices (n_e and n_o) of the LCs [(1) and (2)]. The distance over which the molecules rotate 360° is called *P*.

$$\lambda = P \times n \tag{1}$$

$$\Delta\lambda = P \times \Delta n \tag{2}$$

Here: n is the average refractive index of the film and Δn is the birefringence ($n_e - n_o$).

CNC which can form chiral nematic phases have been investigated by Wang et al. for optical display applications (Wang et al. 2008). They observed that liquid crystallinity of CNC suspensions coupled to the birefringent nature of the particles, leads to interesting optical phenomena. As the lyotropic LC onset concentration is reached, the particles align creating a macroscopic birefringence. Though it is extremely difficult to align and preserve the chiral nematic structure in films of LCs, if suitably stabilized, CNCs can preserve this structure upon drying to a thick film resulting in parabolic focal conic defect structures that are reminiscent of smectic and lamellar LCs of polymers and lipids (Saito et al. 2007) In this case, the chiral structure pitch determines size scales and results in dazzling optical displays as seen in Fig. 9.25. When the reflection wavelength of cholesteric LC is in the range of visible light, well oriented layers of the cholesteric LCs give rise to vivid iridescent colors and the color is angular dependent. For these reasons cholesteric LCs are being investigated for application as special pigments in paints. Because the reflected light is circularly polarized, the materials are also suitable for the preparation of polarization-sensitive optical components.

Chiral nematic LCs are gaining popularity in electrically switchable devices because of the improved colour, brightness and other enhanced properties it can offer. The devices are known as surface stabilized cholesteric texture devices and are of particular interest in applications that require good viewing angles and high brightness.

Another remarkable potential application of transparent CNC-templated material is its utilization in cholesteric-based mirrorless lasing (Finkelmann et al. 2001; Palffy-Muhoray et al. 2006). Recent work has confirmed that the combination of solidified cholesteric LC films with different pitch values with an intermediate film of non-chiral low molar mass nematic can produce broadband (essentially white light) cavity mode lasing with tunability offered by the switchable nematic layer

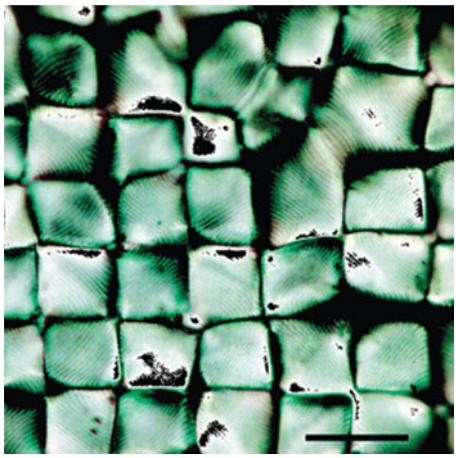

Fig. 9.25 Parabolic focal conics in CNCs viewed between crossed polarizers. Reprinted with permission from Roman and Gray (2005). Copyright American Chemical Society

(Takezoe 2010). Takanishi et al. proved that the combination of multiple solidified cholesteric layers can reduce the lasing threshold spectacularly (Takanishi et al. 2010).

It is remarkable that the phenomenon of transient electric birefringence effect is observed in CNC dispersions in both water as well as organic solvents. The outstanding properties which resulted offer the prospective to extend the aforementioned phenomenon to a variety of devices which are of tremendous efficacy in the present scenario such as: display technology superior to current TFT-LCD displays; variable density optical filters; light valves etc. The dielectric anisotropy of CNCs is positive, and an electric field thus acts to unwind the helix. It was reported that uniform CNC alignment in films obtained by drying CNC suspensions in the presence of electric fields with frequencies in the kHz–MHz range and an amplitude of B2 kV cm^{-1} (Habibi et al. 2008).

Inorganic materials are preferred in lasing applications when exposed to high intensity lights, due to their superior stability and life time compared to that of the organic counterparts. Cholesteric CNC suspensions have recently been used as templates to produce inorganic films with an internal left-handed helical structure (Shopsowitz et al. 2011, 2012). CNC templated films were produced by adding inorganic sol–gel precursors such as tetra methyl orthosilicate or 1, 2-bis (trimethoxysilyl) ethane and simply allowing a certain amount of the suspension to dry under ambient conditions in a Petri dish. The CNC self-assembles into a cholesteric phase as the concentration increases in the precursor solution, and the resulting film after solidification and calcination or acid treatment obtains an internal structure that is a replica of the CNC helix. CNC template method produces inorganic materials with helical structure same that of the CNC material, the templating method is schematically given in Fig. 9.26.

Generally, the helical P of the CNC-inorganic composite before calcination is larger than visible light wavelengths, and the initial composite film therefore shows

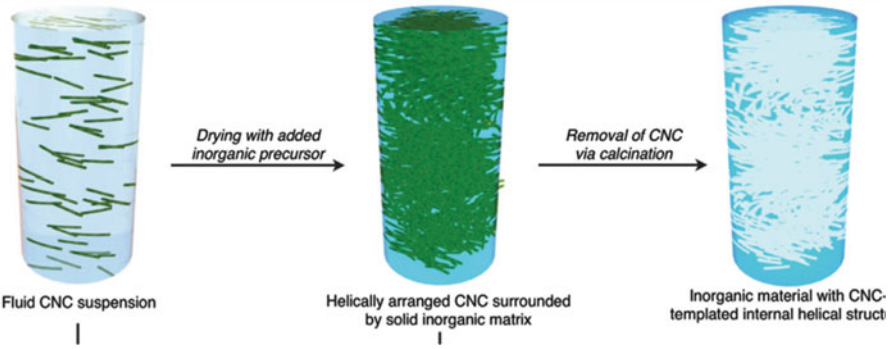

Fig. 9.26 Schematic illustration of the CNC-templating of inorganic materials. Fluid CNC suspension (*left*), which may be liquid crystalline or isotropic added with an inorganic precursor is dried to form CNC helix contained in an inorganic solid matrix (*middle*). By calcinating the sample, the CNCs are removed, leaving the inorganic material with a CNC-templated internal helical structure (*right*). Reproduced with permission from Shopsowitz et al. (2012). Copyright ACS 2013

no color. However, after the cellulose has been removed, the remaining inorganic film frequently shows visible Bragg reflection and the resulting characteristic iridescent colors. SEM investigations in these cases revealed that the removal of the CNCs leads to a compression of the helical structure such that the periodicity is small enough that the photonic band gap falls within the visible range. Films templated from CNCs are attractive because they combine the high surface area of mesoporous materials with the long-range ordering of LCs, specifically with the helical arrangement of the chiral nematic phase. Following this approach one can thus endow any inorganic material that can be templated from a CNC suspension with photonic crystal properties, with visible Bragg reflection if the pitch is in the range of a few hundred nm.

Another important work associated with the field of LC is the synthesis of polymer composites with chiral nematic photonic structures through the self-assembly of CNC dispersions in organic solvents (Clement et al. 2013). Upon neutralization of CNC-H with various strong bases and freeze-drying, Clement and coworkers were able to easily prepare dispersions of CNC-X ($X = Li^+, Na^+, K^+, NH^{4+}, NMe^+, NBu^{4+}$) in polar organic solvents including DMSO, formamide, N-methylformamide, or DMF using stirring and mild sonication. Commodity polymers, such as polystyrene (PS), poly(methyl methacrylate) (PMMA), polycarbonate (PC), and poly(9-vinylcarbazole) (PVK), are soluble in DMF and hence composite materials can be readily prepared using these polymers as matrix. Mixing these polymers with CNC-Na dispersions (3.5 wt%) in DMF followed by slow evaporation of the solvent is a facile way to prepare iridescent composite films with chiral nematic structure The self-assembly of the organic CNC dispersions can be exploited to prepare iridescent polymeric composites simply by casting the CNC dispersion with a suitable polymer soluble in the organic solvent. This depicts a versatile method to generate new iridescent polymer composites with chiral

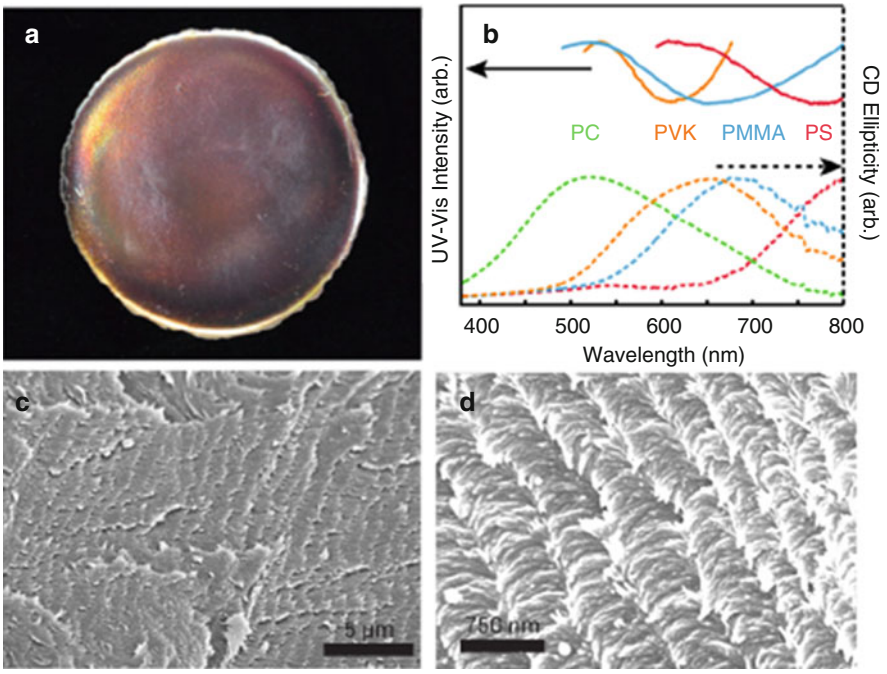

Fig. 9.27 (**a**) Photograph of an iridescent CNC-Na/PMMA composite film with chiral nematic ordering. (**b**) UV–vis and CD spectra of composites with 46 wt% polymer prepared with PS, PMMA, PC, and PVK (UV–vis spectrum of CNC-Na/PC is omitted because of strong absorption of the polymer around the reflected wavelength). (**c**) Representative SEM image of a CNC-Na/PC composite demonstrating the periodic layered structure. (**d**) At higher magnification, SEM shows the left-handed helical morphology of the spindle-shaped CNCs (Reproduced with permission from Clement et al. (2013). Copyright ACS 2013)

nematic structures by successfully dispersing neutralized CNC in polar organic solvents such as DMF. This approach is easily scalable to obtain large area thin films and coatings that could be used for applications such as reflective filters. It is anticipated that the general method of using organic dispersions of CNC as a chiral nematic template will pave the way to an expansive array of new photonic composites or mesoporous materials (Fig. 9.27).

9.5 Conclusions and Future Prospects

The study of LCs is an attractive research field that has engrossed significant curiosity and their synthesis from natural sources has awakened quite an enormous deal of scientific awareness. This is largely because of the vast prospective combined with the capacity for self-assembly of renewable materials like CNCs, natural oils etc. Interdisciplinary research in engineering, biology, physics, medicine, and

chemistry will be crucial for taking LC research to further heights and new applications and to provide a consistent understanding of these fascinating particles. The exploration of these molecular materials is still a challenge since the rapid development of display technology demands new LC materials, which possess as wide a range of properties as possible. Nanostructured films with a photonic band gap arising from the spontaneous helix formation in the cholesteric LC phase of CNC suspensions have been the emphasis of several studies in the current scenario and it is anticipated that this field will be the focus of serious research which will undeniably lead to diverse applications in the days to come. The exploitation of a CNC suspension as a self-assembled template for the synthesis of inorganic materials that adopt the CNC-derived periodic internal structure undoubtedly offers a promising and versatile platform for fabricating multifunctional mesoporous materials with photonic crystal properties and very large surface areas. The utilization of other inorganic materials with higher refractive indices may be predominantly remarkable for photonic devices such as tunable mirrorless lasers, and CNC-templated materials with specific surface functionalities may pave the way for the development of enantioselective sensors (Lagerwall et al. 2014). Furthermore, an analogous templating route could be utilized to fabricate sturdy and fracture resistant composite materials with a helical internal structure derived from CNC, that mimic many industrially useful and potential high-performance biomaterials such as lobster cuticle (Nikolov et al. 2010). Vital issues dealing with the sensitive balance between LC formation and gelation/glass formation have yet to be fully understood. It is seen that are both promoted by the high aspect ratio of CNC rods. In particular, when cholesteric structures with a short and highly specified pitch are desired, primarily for photonic devices, one must develop a means of handling the transition into a non equilibrium glassy state, as this becomes increasingly likely at the high CNC concentrations required for a short-pitch helix. To this end, controlled drying and alternative solvent removal strategies are of interest. Another possible approach to improving the control of the helical self-assembly could be to vary the atmospheric humidity during evaporation or to add a nonvolatile co-solvent (Zhang et al. 2008). Probably the most compelling direction of research into these systems seeks to understand the possibility of controlling the alignment of CNCs, in helical or non-helical states. Large-scale uniform alignment with control of the director and/or helix axis orientation has been made possible by using appropriately designed nano patterned substrates and/or subjecting the drying CNC suspension to appropriately selected mechanical, electrical or magnetic fields. Such control also deserves additional awareness and is indeed an essential prerequisite for quite a lot of significant applications such as lasers, security papers and certain sensors. Attempts to decrease the length distribution of CNCs sounds promising, as this could lead not only to the manifestation of smectic and/or columnar phases of CNCs, which are of primary concern, but also to other applications in nanostructured and ordered composite materials. The attractive optical properties of this self-assembled bio-derived photonic crystal have inspired several attempts to utilize CNC films in novel applications such as optical encryption 15 or as chiral templates.

Investigations of biologically inspired liquid crystalline structures will improve the understanding of the relation between the structure, functions and LC phases and may possibly lead to the recipes of creating super strength materials and may throw some light into the mechanisms of biological functions. As a conclusion we would like to comment that bio-inspired LCs/LCPs are a better way to future materials as it combines self-assembly, enhanced properties and functions and importantly eco-friendliness in the same package.

References

Abid S, Gharbi RE, Gandini A (2004) Polyamides incorporating furan moieties. Synthesis and characterization of furan-aromatic homologues. Polymer 45:5793–5801

Al-Bawab A, Heldt N, Li Y (2005) Emulsified orange oil in an aqueous vesicle solution. J Dispers Sci Technol 26:251–256

Almgren M (1980) Migration of Pyrene between lipid vesicles in aqueous solution. A stopped-flow study. Chem Phys Lett 71(3):539–543

Araki J, Wada M, Kuga S, Okano T (2000) Birefringent glassy phase of a cellulose microcrystal suspension. Langmuir 16:2413–2415

Azizi Samir MAS, Alloin F, Dufresne A (2005) Review of recent research into cellulosic whiskers, their properties and their application in nanocomposite field. Biomacromolecules 6:612–626

Bajpai UDN, Nivedita NP (1996) Cheremision off multiphase reactor and polymerization system hydro-dynamics; advances in engineering fluid mechanics series. Gulf Publishing Company, Houston, p 583

Beck R, Deek J, Jones JB, Safinya CR (2009) Gel-expanded to gel-condensed transition in neurofilament networks revealed by direct force measurements. Nat Mater 9:40–46

Beck R, Deek J, Choi MC, Ikawa T, Watanabe O, Frey E, Pincus PA, Safinya CR (2010a) Unconventional salt-switch from soft to stiff in single neurofilament biopolymers. Langmuir 26:18595–18599

Beck R, Deek J, Jones JB, Safinya CR (2010b) Gel expanded–gel condensed transition in neurofilament networks revealed by direct force measurements. Nat Mater 9:40–46

Beck S, Bouchard J, Chauve G, Berry R (2013) Controlled production of patterns in iridescent solid films of cellulose nanocrystals. Cellulose 20:1401–1411

Belamie E, Mosser G, Gobeaux F, Giraud-Guille MM (2006) Possible transient liquid crystal phase during the laying out of connective tissues: α-chitin and collagen as models. J Phys Condens Matter 18:S115

Bouligand Y (2008) Liquid crystals and biological morphogenesis: ancient and new questions. C R Chim 11:281–296

Ching G, Liem RJ (1993) Assembly of type IV neuronal intermediate filaments in nonneuronal cells in the absence of preexisting cytoplasmic intermediate filaments. J Cell Biol 122:1323–1335

Choi MC, Raviv U, Miller HP, Gaylord MR, Kiris E, Ventimiglia D, Needleman DJ, Kim MW, Wilson L, Feinstein SC, Safinya CR (2009) Human microtubule-associated-protein tau regulates the number of protofilaments in microtubules: a synchrotron X-ray scattering study. Biophys J 97:519–527

Clement CY, Cheung MG, Kelly JA, Hamad WY, MacLachlan MJ (2013) Iridescent chiral nematic cellulose nanocrystal/polymer composites assembled in organic solvents. ACS Macro Lett 2(11):1016–1020

Davidson P, Gabriel J-CP (2005) Mineral liquid crystals. Curr Opin Colloid Interface Sci 9 (2005):377–383

Davidson MW, Strzelecka TE, Rill RL (1998) Multiple liquid crystal phases of DNA at high concentrations. Lett Nat 331:457–460

Deek J, Chung PJ, Kayser J, Bausch AR, Safinya C (2013) Neurofilament sidearms modulate parallel and crossed-filament orientations inducing nematic to isotropic and re-entrant birefringent hydrogels. Nat Commun 4:2224

Dong XM, Kimura T, Revol JF, Gray DG (1996a) Effects of ionic strength on the isotropic-chiral nematic phase transition of suspensions of cellulose crystallites. Langmuir 12:2076–2082

Dong XM, Kimura T, Revol JF, Gray DG (1996b) Effects of ionic strength on the phase separation of suspensions of cellulose crystallites. Langmuir 12:2076–2082

Dong Y, Wu Y, Wang J, Wang M (2001) Influence of degree of etherification of critical liquid crystal behavior of hydroxyl propyl chitosan. Eur Polym J 37:1713–1720, Elsevier

Ebeling T, Paillet M, Borsali R, Diat O, Dufresne A, Cavaille JY, Chanzy H (1991) Shear-induced orientation phenomena in suspensions of cellulose microcrystals, revealed by small angle X-ray scattering. Langmuir 15:6123–6126

Elliott A, Ambrose EJ (1950) Discuss Faraday Soc 9:246

Ewert KK, Evans HM, Zidovska A, Bouxsein NF, Ahmad A, Safinya CR (2006) A columnar phase of dendritic lipid-based cationic liposome-DNA complexes for gene delivery: hexagonally ordered cylindrical micelles embedded in a DNA honeycomb lattice. J Am Chem Soc 128:3998–4006

Finkelmann H, Kim ST, Munoz A, Palffy-Muhoray P, Taheri B (2001) Tunable mirrorless lasing in cholesteric liquid crystalline elastomers. Adv Mater 13:1069–1072

Fleming K, Gray DG, Matthews S (2001) Cellulose crystallites. Chemistry 7:1831–1835

Folda T, Hoffman H, Chanzy H, Smith P (1998) Iquid-crystalline suspensions of. Poly(tetrafluoroethylene) whiskers. Nat Nanotechnol 333:55–56

Fuchs E, Cleveland DW (1998) A structural scaffolding of intermediate filaments in health and disease. Science 279:514–519

Giasson J (1995) Etúdes microscopiques d'hélicoïdes de systè mes cellulosiques in vitro (Chapter 5). Dissertation, McGill University, p 167

Giraud-Guille MM (1992) Liquid crystallinity in condensed type I collagen solutions. A clue to the packing of collagen in extracellular matrices. J Mol Biol 1992(224):861–873

Giraud-Guille MM, Mosser G, Belamie E (2008) Liquid crystallinity in collagen systems in vitro and in vivo. Curr Opin Colloid Interface Sci 13:303–313

Gray DG (1995) Chiral nematic ordering of polysaccharides. Carbohydr Polym 25(4):277–284

Habibi Y, Heim T, Douillard R (2008) AC electric field-assisted assembly and alignment of cellulose nanocrystals. J Polym Sci B Polym Phys 46:1430–1436

Hesse HC, Beck R, Ding C, Jones JB, Deek J, MacDonald NC, Li Y, Safinya CR (2008) Direct imaging of aligned neurofilament networks assembled using in situ dialysis in microchannels. Langmuir 24:8397–8401

Hirai A, Inui O, Horii F, Tsuji M (2009) Phase separation behavior in aqueous suspensions of bacterial cellulose nanocrystals prepared by sulfuric acid treatment. Langmuir 25:497–502

Hirst LS, Pynn R, Bruinsma RF, Safinya CR (2005) Hierarchical self-assembly of actin bundle networks: gels with surface protein skin layers. J Chem Phys 123:104902

Hou HQ, Reuning A, Wendorff JH, Greiner A (2000) Tuning of pitch height in thermotropic cellulose esters. Macromol Chem Phys 201:2050–2054

Huang Y, Liang W, Shen JR (1995) Molecular interactions and formation of lyotropic liquid crystals of hydroxyethyl cellulose acetate. Polymer Bulletin 35:357–364

Huang B (2007) Aliphatic acid esters of (2-hydroxypropyl) cellulose—effect of side chain length on properties of cholesteric liquid crystals. Polymer 48(2007):264–269

Jana NR (2004) Shape effect in nanoparticle self-assembly. Angew Chem Int Ed Engl 43:1536–1540

John G, Vemula PK (2006) Design and development of soft nanomaterials from biobased amphiphiles. Soft Matter 2:909–914

Jones JB, Safinya CR (2008) Interplay between liquid crystalline and isotropic gels in self-assembled neurofilament networks. Biophys J 95:823–825

Kerkam K, Viney C, Kaplan DL, Lombardi S (1991) Liquid crystalline characteristics of *natural* silk secretions. Nature 349:596–598

Khare K, Tiwari S, Reddy KV, Bajpai A, Nagaraju V (2013) Study of liquid-crystalline behaviour of aliphatic-aromatic polyamides derived from castor oil based dimer acid by DSC. Indian J Adv Chem Sci 2(1):89–94

Kim I et al (2009) Liquid crystal O/W emulsions to mimic lipids and strengthen skin barrier function. Cosm Toil

Klemm D, Heublein B, Fink HP, Bohn A (2005) Cellulose: fascinating biopolymer and sustainable raw material. Angew Chem Int Ed Engl 44:3358–3393

Knight DP, Vollrath F (2002) Spinning an elastic ribbon of spider silk. Philos Trans R Soc Lond B Biol Sci 357(1418):219–227

Koltover I, Salditt T, Rädler JO, Safinya CR (1998) An inverted hexagonal phase of cationic liposome-DNA complexes related to DNA release and delivery. Science 281:78–81

Lagerwall JPF, Schütz C, Salajkova M, Noh JH, Park JH, Scalia G, Bergström L (2014) Cellulose nanocrystal-based materials: from liquid crystal self-assembly and glass formation to multifunctional thin films. NPG Asia Mater 6:e80

Lee AG (1997) Lipid phase transitions and phase diagrams. I. Lipid phase transitions. Biochim Biophys Acta 472:237–281

Luzzati V, Cesari M, Spach G, Masson F, Vincent B (1961) The structure of L-poly-gamma-benzyl glutamate in solution. Configuration of a helix different from helix alpha and transitions between helical forms. J Mol Biol 3:566–584

Majoinen J, Kontturi E, Ikkala O, Gray DG (2012) SEM imaging of chiral nematic films cast from cellulose nanocrystal suspensions. Cellulose 19:1599–1605

Moon RJ, Martini A, Nairn J, Simonsen J, Youngblood J (2011) Cellulose nanomaterials review: structure, properties and nanocomposites. Chem Soc Rev 40:3941–3994

Needleman DJ, Ojeda-Lopez MA, Raviv U, Miller HP, Wilson L, Safinya CR (2004) Higher-order assembly of microtubules by counterions: from hexagonal bundles to living necklaces. Proc Natl Acad Sci U S A 101:16099–16103

Needleman DJ, Jones JB, Raviv U, Ojeda-Lopez MA, Miller HP, Li Y, Wilson L, Safinya CR (2005) Supramolecular assembly of biological molecules purified from bovine nerve cells: from microtubule bundles and necklaces to neurofilament networks. J Phys Condens Matter 17:3225

Nikolov S, Petrov M, Lymperakis L, Friak M, Sachs C, Fabritius H, Raabe D, Neugebauer J (2010) Revealing the design principles of high-performance biological composites using ab initio and multiscale simulations: the example of lobster cuticle. Adv Mater 22:19–526

Onsager L (1949) Effects of shape on the interaction of colloidal particles. Ann N Y Acad Sci 51:627–659

Oster G (1950) Two phase formation in solutions of tobacco mosaic virus and the problem of long range forces. J Gen Physiol 33:445–473

Palffy-Muhoray P, Cao W, Moreira M, Taheri B, Munoz A (2006) Photonics and lasing in liquid crystal materials. Philos Transact A Math Phys Eng Sci 364:2747–2761

Rädler JO, Koltover I, Salditt T, Safinya CR (1997) Structure of DNA-cationic liposome complexes: DNA intercalation in multilamellar membranes in distinct interhelical packing regimes. Science 275:810–814

Rathore O, Sogah DY (2001) Self-assembly of beta-sheets into nanostructures by poly(alanine) segments incorporated in multiblock copolymers inspired by spider silk. J Am Chem Soc 123:5231–5239

Revol JF, Bradford H, Giasson J, Marchessault RH, Gray DG (1992) Helicoidal self-ordering of cellulose microfibrils in aqueous suspension. Int J Biol Macromol 1992(14):170–172

Revol J-F, Godbout JDL, Gray DG (1995) International Patent WO 95/21901

Robinson C (1966) The cholesteric phase in polypeptide solutions and biological structures. Mol Cryst 1:467–494
Roman M, Gray DG (2005) Parabolic focal conics in self-assembled solid films of cellulose nanocrystals. Langmuir 21:5555–5561
Safinya CR (2006) Biophysics and biomaterials. In: Fraser G (ed) The new physics for the twenty-first century. Cambridge University Press, Cambridge
Safinya CR, Liang KS, Varady WA, Clark NA, Andersson G (1984) Synchrotron X-ray study of the orientational ordering D2-D1 structural phase transition of freely suspended discotic strands in triphenylene-hexa-dodecanoate. Phys Rev Lett 53:1172–1175
Safinya CR, Raviv U, Needleman DJ, Zidovska A, Choi MC, Ojeda-Lopez MA, Ewert KK, Li Y, Miller HP, Quispe J, Carragher B, Potter CS, Kim MW, Feinstein SC, Wilson L (2011) Nanoscale assembly in biological systems: from neuronal cytoskeletal proteins to curvature stabilizing lipids. Adv Mater 23:2260–2270
Saito T, Kimura S, Nishiyama Y, Isogai A (2007) Cellulose nanofibers prepared by TEMPO mediated oxidation of native cellulose. Biomacromolecules 8:2485–2491
Saminathan M, Pillai CKS (2000) Synthesis of novel liquid crystalline polymers with cross-linked network structures. Polymer 41:3103–3108
Shopsowitz KE, Qi H, Hamad WY, MacLachlan MJ (2010a) Free-standing mesoporous silica films with tunable chiral nematic structures. Nature 2010(468):422–426
Shopsowitz KE, Qi H, Hamad WY, MacLachlan MJ (2010b) Free-standing mesoporous silica with tunable chiral nematic structures. Nature 468:422–426
Shopsowitz KE, Hamad WY, MacLachlan MJ (2011) Chiral nematic mesoporous carbon derived from nanocrystalline cellulose. Angew Chem Int Ed 50:10991–10995
Shopsowitz KE, Stahl A, Hamad WY, MacLachlan MJ (2012) Hard templating of nanocrystalline titanium dioxide with chiral nematic ordering. Angew Chem Int Ed Engl 51:6886–6890
Stegemeyer H (1999) Lyotrope flussigkristalle: grundlagen, entwicklung, anwendung. Steinkopff/Springer-Verlag, Darmstadt/Berlin
Swatloski RP, Spear SK, Holbrey JD, Rogers RD (2002) Dissolution of cellulose with ionic liquids. J Am Chem Soc 124:4974–4975
Takanishi Y, Ohtsuka Y, Suzaki G, Nishimura S, Takezoe H (2010) Low threshold lasing from dye-doped cholesteric liquid crystal multi-layered structures. Opt Express 18:12909–12914
Takezoe H (2010) Broadband cavity-mode lasing from dye-doped nematic liquid crystals sandwiched by broadband cholesteric liquid crystal bragg reflectors. Adv Mater 22:2680–2684
Tseng SL, Laivins GV, Gray DG (1982) Esterification of 2-hydroxypropyl cellulose (HPC). Macromolecules 15:1262–1264
Unger EC, Lund PJ, Shen DK, Fritz TA, Yellowhair D, New TE (1992) Nitrogen-filled liposomes as a vascular US contrast agent: preliminary evaluation. Radiology 185(2):453–456
Van Winkle DH, Clark NA (1982) Freely suspended strands of tilted columnar liquid crystal phases: one dimensional nematics with orientational jumps. Phys Rev Lett 48:1407–1410
Wang N, Ding E, Cheng RS (2008) Preparation and liquid crystalline properties of spherical cellulose nanocrystals. Langmuir 24(1):5–8
Zhang Y, Yang S, Chen L, Evans JRG (2008) Shape changes during the drying of droplets of suspensions. Langmuir 24:3752–3758
Zidovska A, Evans HM, Ewert KK, Quispe J, Carragher B, Potter CS, Safinya CR (2009) Liquid crystalline phases of dendritic lipid–DNA self-assemblies: lamellar, hexagonal and DNA bundles. J Phys Chem B 113:3694–3703